Systematic study of 1*s*-*ns* and 1*s*-*nd* two-photon transitions of hydrogenlike atoms

Viorica Florescu, Suzana Pătrascu, and O. Stoican
Faculty of Physics, University of Bucharest, P.O. Box 5211, Bucharest-Magurele 76900, Romania
(Received 5 September 1986; revised manuscript received 16 April 1987)

We present the results of a numerical study of the invariant amplitudes of 1*s*-*ns* and 1*s*-*nd* two-photon transitions in hydrogenlike atoms in the nonrelativistic dipole approximation, based on compact analytic formulas. We report also results valid in the limit $n \to \infty$. The 1*s*-*nd* transitions with $n > 6$ are studied for the first time. For other particular cases our numerical results are in agreement with previous calculations in the literature. The investigated energy region of the two-photon spectrum is extended. The position of the transparencies in the second half of the spectrum is found to be almost n independent.

I. INTRODUCTION

Two-photon transitions in hydrogenlike atoms have been explored in a large number of papers. The 1*s*-*ns* transition plays a special role, because this transition determines the lifetime of the metastable 2*s* state.[1] In usual experimental conditions other two-photon transitions are in competition with one-photon transitions.

The existing works on two-photon transitions have used different analytical and numerical procedures. We mention here some of the previous results. After studying the 1*s*-2*s* transition with the Green's-function method, Zon *et al.*[2] have derived analytic expressions for several bound-bound two-photon transitions in terms of Gauss functions. At the same time bound-free two-photon transitions were studied independently by Gavrila,[3] Klarsfeld,[4] and Rapoport *et al.*[5] Using the Sturmian expansion of the Coulomb Green's function, Karule[6] has obtained general expressions for the Nth-order bound-bound and bound-free transitions, for any $N \geq 2$. Formulas describing bound-bound two-photon transitions between arbitrary hydrogenic states were considered in a paper by Gazeau,[7] but to our knowledge they were not used in a numerical study. Much more attention continues to be paid to bound-free transitions.[8–10]

Our purpose here is to contribute to a detailed knowledge of the properties of 1*s*-*ns* and 1*s*-*nd* two-photon transitions with $n > 2$ in hydrogenlike atoms. Previous works with the same purpose are reported in Refs. 11–13.

Quattropani *et al.*[11] have studied in detail two-photon absorption in 1*s*-*ns* transitions. They have presented precise numerical results for several values of n ($n = 3$, 6, 20, and 45). Photon transparencies and the behavior of the transition rates for large values of n (extrapolation to $n \to \infty$) have been presented. The analytical formulas used are nevertheless complicated. Working in both velocity and length gauges, precision was controlled in a satisfactory way.

Tung *et al.*[12] have studied for the first time some properties of the 1*s*-*nd* transitions. Their work, which treats the cases $3 \leq n \leq 6$ (both *ns* and *nd*) is based on analytical expressions for the transition amplitudes. An independent calculation[13] for the $1s \leftrightarrow 3s, 3d$ cases is in full agreement with the results reported in Refs. 11 and 12. It is based on a simple analytic expression for the Kramers-Heisenberg matrix element.

Recently,[14] in connection with the treatment of the linear response of the hydrogen atom to an external

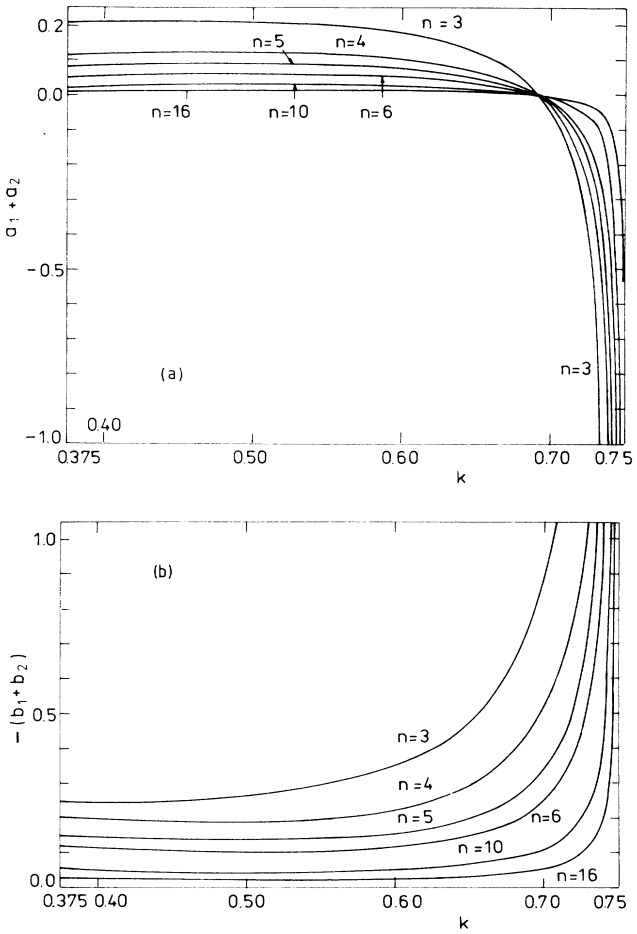

FIG. 1. (a) The amplitude $a_1 + a_2$ of the 1*s*-*ns* transitions for several values of n, as a function of k for $0.375 < k < 0.75$. (b) The amplitude $-(b_1 + b_2)$ of the 1*s*-*nd* transitions, in the same conditions as in (a).

one-mode electromagnetic field, compact analytic expressions for the amplitudes of $1s$-ns and $1s$-nd two-photon transitions were derived. This method of calculation was mention earlier by Luban and co-workers,[15] but the results were never published. The formulas obtained in this way contain Appell functions F_1 which reduce to a finite number of Gauss functions. It appears that these equations can be connected with those given by Arnous *et al.*[9] for $1s$ two-photon ionization. We mention also a recent analytic work[16] oriented toward the simplification of the analytic expression of two-photon transition amplitudes, based on a technique of reducing the number of Gauss functions to only one.

Besides its intrinsic interest, the study of the hydrogenlike case served in the past to lead to qualitative understanding of two-photon transitions in many-electron atoms, as shown by Freund.[17] Double-photon decay has been observed in atoms with a K-shell vacancy, molybdenum atoms in the experiment of Bannett and Freund,[18] and xenon atoms in the study of Ilakovac and coworkers.[19] The two-photon spectrum was analyzed in the last paper in terms of transitions from $2s$, $3s$, $3d$, and $4s$ states. The experiments reveal a more complex situation than in the hydrogenic model. The results of the first relativistic self-consistent-field calculation of two-photon bound-bound transitions for xenon have been published very recently.[20]

In this paper we present the results of a systematic study of the amplitudes for the $1s$-ns and $1s$-nd transitions with $n \geq 3$, based on analytic formulas in terms of F_1 functions. In Sec. II we present the analytic formulas we use together with particular simple expressions valid at the end of the spectrum. The analytic results valid for $n \rightarrow \infty$ are given in Sec. III. The conclusions of the numerical calculations are reported in Sec. IV as graphs. A table with the energies of the transparencies is also given. Some relations used in the analytical or numerical work are given in Appendixes.

II. ANALYTIC EXPRESSIONS FOR THE INVARIANT AMPLITUDES

Our study of two-photon $1s$-ns and $1s$-nd transitions in hydrogenlike atoms is based on an analytic technique, developed in Ref. 14, for the evaluation of the Kramers-Heisenberg matrix element. This matrix element for arbitrary initial and final states is

$$\mathcal{M}_{i,f} = -[\Pi_{jk;i,f}(\Omega_1) + \Pi_{kj;i,f}(\Omega_2)] s_{1k} s_{2j} \ , \tag{1}$$

where s_{1k} and s_{2j} are the Cartesian components of the polarization vectors of the photons in the absorption case, or their complex conjugate in the emission case, and

$$\Pi_{jk;i,f}(\Omega) \equiv \frac{1}{m_e} \langle f \mid P_k \mid w_{j;i}(\Omega) \rangle \ , \tag{2}$$

with

$$\mid w_{j;i}(\Omega) \rangle = G(\Omega) P_j \mid i \rangle \ . \tag{3}$$

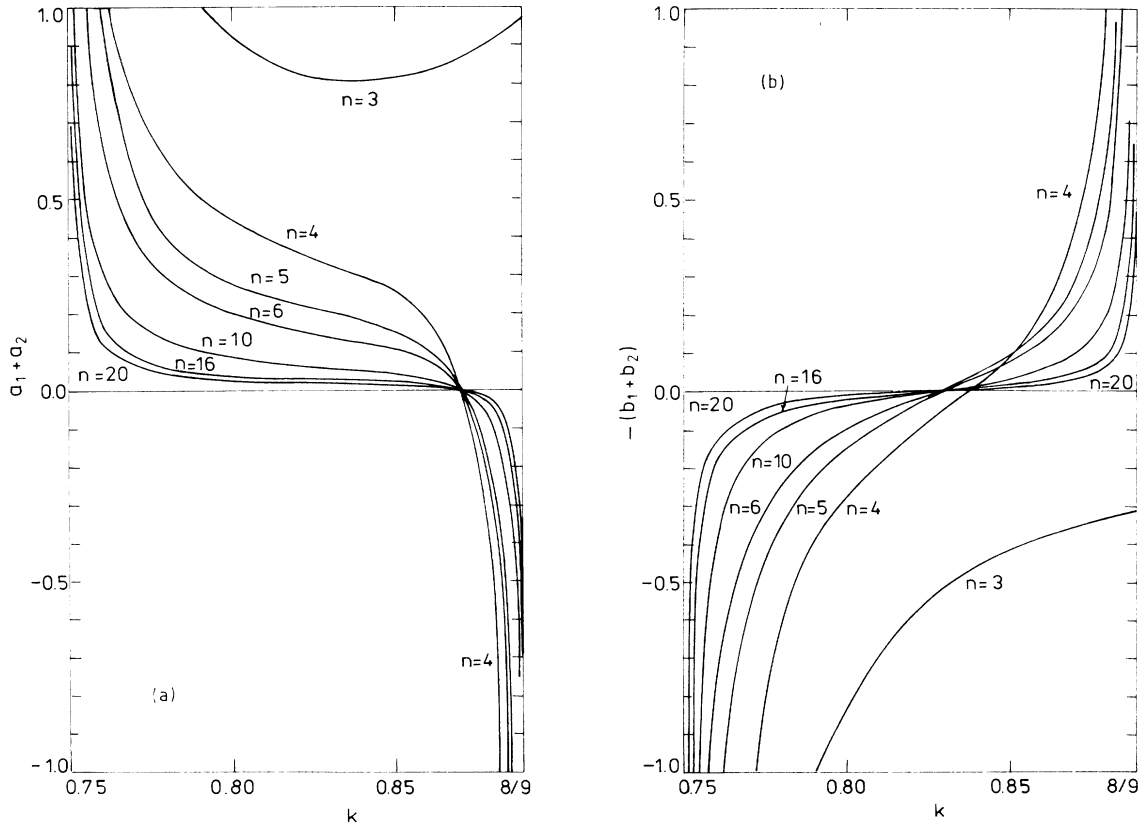

FIG. 2. (a) Same as 1(a), but for $0.75 < k < 0.8889$. (b) Same as 1(b), but for $0.75 < k < 0.8889$.

P is the momentum operator, G the resolvent operator for the Coulomb field, m_e the electron mass; Ω_1,Ω_2 will be specified further. The knowledge of the vectors (3) allows a straightforward evaluation of the Kramers-Heisenberg matrix element. The same vectors determine the linear response of the atomic state i to a one-mode electromagnetic field in the dipole approximation.[14,21]

Given two atomic states i and f with $E_i < E_f$, the matrix element (1) corresponds to the absorption of two photons of energies $\hbar\omega_1$ and $\hbar\omega_2$ connected by

$$\hbar\omega_1+\hbar\omega_2=E_f-E_i \tag{4}$$

if one takes

$$\Omega_\alpha=E_i+\hbar\omega_\alpha,\quad \alpha=1,2\ . \tag{5}$$

The matrix element $\mathcal{M}_{f,i}$ (with $\mathbf{s}_{1,2}\rightarrow\mathbf{s}^*_{2,1}$) describes two-photon emission if Ω_1 and Ω_2 interchange their roles. Due to the Hermitian properties of **P** and G, one has the relation $\mathcal{M}_{f,i}=(\mathcal{M}_{i,f})^*$.

The connection between the matrix element and the measurable quantities is shown in Sec. IV.

Here we study only the case of $1s$-ns,nd transitions and we refer to the matrix element (1) for the case of absorption, i.e., we use (5) with $E_i=E_1$. The dependence on j and k of the quantity (2) is rather simple in this case:

$$\Pi_{jk;1s,ns}(\Omega)=a(\tau)\delta_{jk}\ , \tag{6}$$

$$\Pi_{jk;1s,n2m}(\Omega)=b(\tau)C^*_{m,jk}\ , \tag{7}$$

where δ_{jk} is the Kronecker symbol and $C_{m,jk}$ the coefficients appearing in the expansion of the spherical harmonics of rank 2 in terms of Cartesian coordinates

$$Y_{2m}(\hat{\mathbf{r}})=\frac{1}{\sqrt{4\pi}}\sum_{j,k}C_{m,jk}x_jx_k/r^2\ .$$

$C_{m,jk}$ are symmetric in j and k. In this way, in Eq. (7) the dependence on the magnetic substate m is specified, too. The functions a and b are the *invariant amplitudes* of $1s$-ns and, respectively, $1s$-nd transitions. The analytic results that follow show that the invariant amplitudes depend on a unique variable τ defined by

$$\tau\equiv\alpha Zm_ec/(-2m_e\Omega)^{1/2}\ , \tag{8}$$

where α is the fine-structure constant, c the velocity of light and Z the nuclear charge. Ω is negative in two-photon bound-bound transitions, and, consequently, τ and the invariant amplitudes are real. With the notation

$$a(\tau_l)\equiv a_l,\quad b(\tau_l)\equiv b_l,\quad l=1,2\ , \tag{9}$$

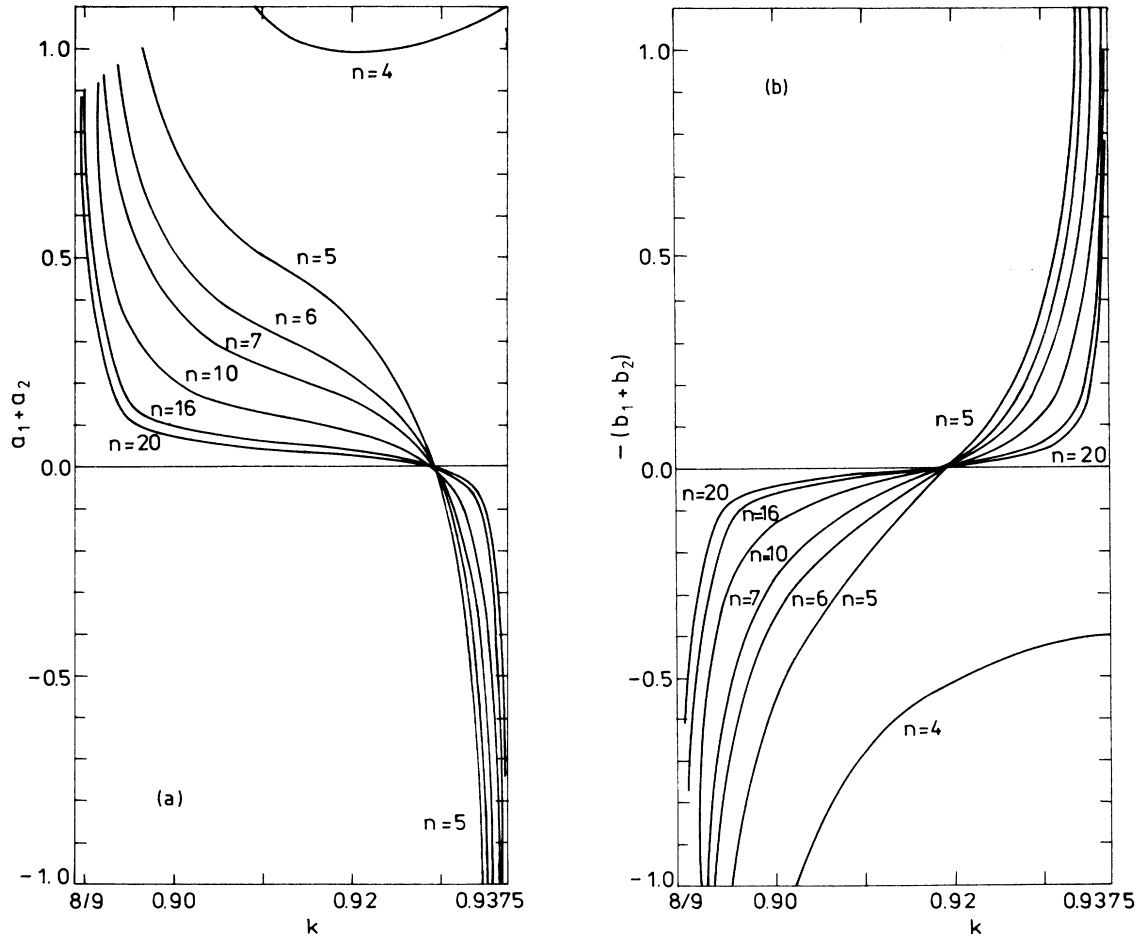

FIG. 3. (a) Same as 1(a), but for $0.8889 < k < 0.9375$. (b) Same as 1(b), but for $0.8889 < k < 0.9375$.

the Kramers-Heisenberg matrix elements we are interested in become

$$\mathcal{M}_{1s,ns} = -(a_1 + a_2)\mathbf{s}_1 \cdot \mathbf{s}_2 \ , \tag{10}$$

$$\mathcal{M}_{1s,nd} = -(b_1 + b_2) C^*_{m,jk} s_{1j} s_{2k} \ . \tag{11}$$

We reproduce now the expressions of the invariant amplitudes a and b used in this work and derived with the method in Ref. 14. With the notation

$$S_j \equiv \frac{1}{1-\tau+j} F_1(1-\tau+j, 3+n, 3-n, 2-\tau+j; x, y) \ , \tag{12}$$

where F_1 is the Appell function (see Appendix A) of the variables

$$x = (1-\tau)(n-\tau)/(1+\tau)(n+\tau) \ ,$$
$$y = (1-\tau)(n+\tau)/(1+\tau)(n-\tau) \ , \tag{13}$$

we have

$$a(\tau) = \frac{2^7 \tau^5 n^{5/2}}{3(1+\tau)^6} \frac{(n-\tau)^{n-3}}{(n+\tau)^{n+3}} \times \{(1+\tau)^2[3\tau^2 - 2\tau(n^2+2) + 3n^2]S_1 - 6(1-\tau^2)(n^2-\tau^2)S_2 + (1-\tau)^2[3\tau^2 + 2\tau(n^2+2) + 3n^2]S_3\} \ , \tag{14}$$

$$b(\tau) = -\frac{2^9 \tau^6 n^{5/2}}{15(1+\tau)^6} (n^2-4)^{1/2}(n^2-1)^{1/2} \frac{(n-\tau)^{n-3}}{(n+\tau)^{n+3}} \times [(1+\tau)^2 S_1 - (1-\tau)^2 S_3] \ . \tag{15}$$

For $n = 3$ we mention the agreement[22] with Ref. 13.

For $|x| < 1$ and $|y| < 1$ the Appell function F_1 can be expressed as a double-series expansion in x and y [see (A1)]. In our problem the third parameter of the Appell functions is a nonpositive integer, so the expansion (A2) contains a finite number of terms and can be used even

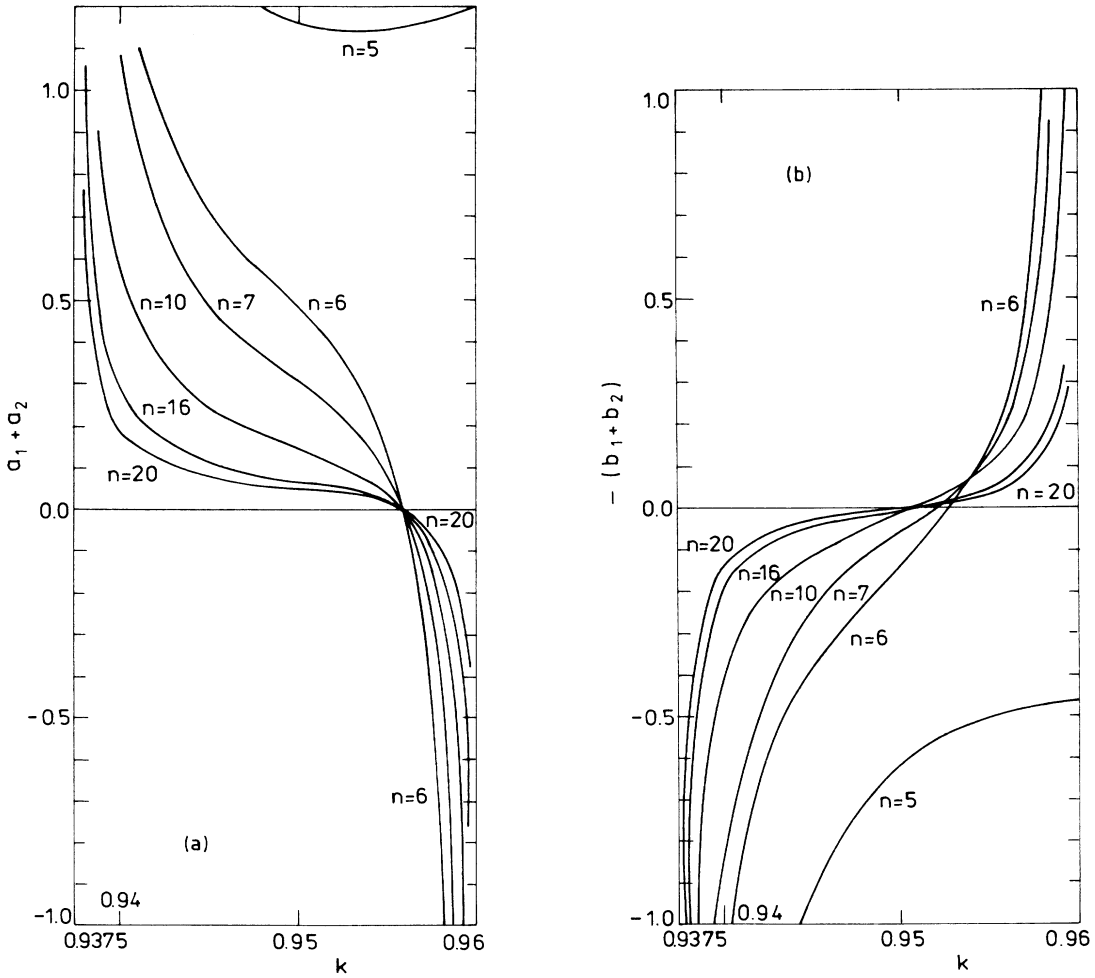

FIG. 4. (a) Same as 1(a), but for $0.9375 < k < 0.96$. (b) Same as 1(b), but for $0.9375 < k < 0.96$.

for $|y|>1$.

The explicit expressions of τ_1 and τ_2 corresponding to Ω_1 and Ω_2 in (5) are

$$\tau_1=(1-k)^{-1/2},\quad \tau_2=\left[\frac{1}{n^2}+k\right]^{-1/2}, \tag{16}$$

where k is the energy of one of the photons, measured in $Z^2\times$ Rydberg units,

$$k\equiv\hbar\omega_1/|E_1| . \tag{17}$$

As k goes from 0 to $1-1/n^2$, τ_1 increases from 1 to n, while τ_2 decreases from n to 1.

The expressions of a and b given here are analytically close to those published by Arnous *et al.*[9] for the amplitudes of two-photon ground-state ionization. In particular, our equation (15) for the amplitude b appears to resemble Eq. (4.7) of Arnous *et al.* for an amplitude denoted by T_{12}. This last amplitude, defined in Eq. (2.6) of Ref. 9, is a partial amplitude referring to 1s-*d* continuum-state transition. It corresponds to the quantity $T_{10,n2}$ defined in our equation (C5) and used in the calculations performed in the length gauge. Some care has to be taken in the comparison of our results with those in Ref. 9, based on the general rules of passage from bound to continuum states, because the results of Arnous *et al.* work for photons of the same energy. The formula connecting b and $T_{10,n2}$ is equation (C4). For $\omega_1=\omega_2=\omega$ it reduces to

$$b(\tau)=\tfrac{1}{3}m_e\omega^2T_{10,n2}(\Omega) ,$$

where the unique value of Ω is $(E_1+E_n)/2$ and τ is given by (8). Our expressions (14) and (15) and those published in Ref. 9 can be compared only for $\omega_1=\omega_2$; one finds agreement if the energy conservation, Eq. (4), with $\omega_1=\omega_2$, is explicitly used.

The Kramers-Heisenberg matrix element [Eqs. (10) and (11)] is symmetric with respect to the middle of the spectrum $k=\frac{1}{2}(1-1/n^2)$. The variable x in (13) is negative and subunitary, while y goes monotonically from 0 to $-\infty$ when τ goes from 1 to n.

For $\tau=1$ and $\tau=n$ the expressions of the amplitudes a and b drastically simplify. For $\tau=1$ one has $x=y=0$ and, consequently, one obtains directly from (14) and (15)

$$a(1)=\frac{2^3}{3}n^{5/2}(n-1)^{n-2}/(n+1)^{n+2} ,$$
$$b(1)=-\frac{2^5}{15}n^{5/2}(n^2-4)^{1/2}(n-1)^{n-5/2}/(n+1)^{n+5/2} . \tag{18}$$

For $\tau=n$ the situation is apparently complicated because in this case the variable x goes to zero, while y goes to $-\infty$. This limit is described in Appendix B. The results, based on (B1)–(B3), are

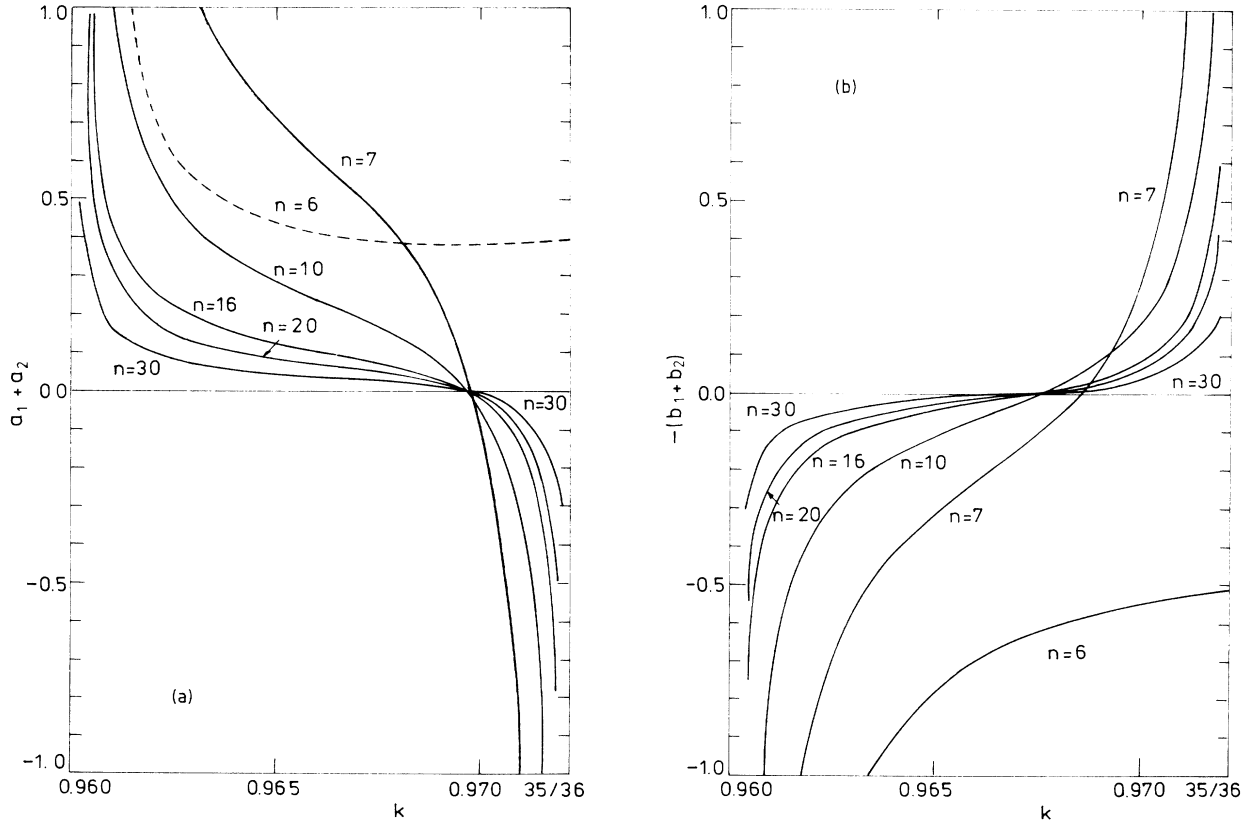

FIG. 5. (a) Same as 1(a), but for $0.96<k<0.972$. For $n=6$ (dashed curve) the function represented is $\frac{3}{10}(a_1+a_2)$. (b) Same as 1(b), but for $0.96<k<0.972$.

$$a(n)=\tfrac{1}{2}(3n^2-5)a(1)\ ,$$
$$b(n)=-\tfrac{1}{4}(3n^2+1)b(1)\ . \tag{19}$$

From (18) and (19) one gets the following results valid at the ends of the spectra ($k=0$ or $k=1-1/n^2$):

$$a_1+a_2\Big|_{k=1-1/n^2}=4n^{5/2}(n-1)^{n-1}/(n+1)^{n+1}\ ,$$
$$b_1+b_2\Big|_{k=1-1/n^2}=\tfrac{8}{5}n^{5/2}(n^2-4)^{1/2}(n-1)^{n-3/2}/(n+1)^{n+3/2}\ . \tag{20}$$

For $\tau=N$ $(1<N<n)$ the amplitudes a and b become infinite if we do not include the finite widths of the energy levels. The behavior in the vicinity of a resonance can be obtained directly from the starting expressions (2) and (3). Some details are given in Appendix C.

III. THE LIMIT OF LARGE VALUES FOR n

For large values of n the invariant amplitudes decrease smoothly as $n^{-3/2}$. In the ns case Quattropani *et al.*[11] have estimated the values of the product of n^3 with the square of the amplitude for $n\to\infty$, for several photon energies,[23] by extrapolating the numerical results obtained for large values of n. From our analytic expressions (14) and (15) we have derived analytic results valid in the limit $n\to\infty$. The calculation of this limit is similar to that performed for Compton scattering amplitudes by Gavrila.[8] Even the results are in a close connection, as is proved by an adequate analysis.[24] The results are

$$\lim_{n\to\infty} n^{3/2}a=\frac{2^3}{3}\frac{\tau}{(1+\tau)^2}\left[\frac{2\tau}{1+\tau}\right]^{\tau}e^{-2\tau}\times[4\tau^2(3-2\tau)T_1-12\tau(1-\tau)T_2+(1-\tau)^2(3+2\tau)T_3]\ , \tag{21}$$

$$\lim_{n\to\infty} n^{3/2}b=\frac{32}{15}\frac{\tau^2}{(1+\tau)^2}\left[\frac{2\tau}{1+\tau}\right]^{\tau}e^{-2\tau}\times[-4\tau^2T_1+(1-\tau)^2T_3]\ , \tag{22}$$

where we have used the notation

$$T_j\equiv\frac{1}{1-\tau+j}\phi_1(1-\tau+j,-4-\tau+j,2-\tau+j;\xi,\eta)\ , \tag{23}$$

with

$$\xi=(\tau-1)/2\tau,\quad \eta=2(\tau-1)\ .$$

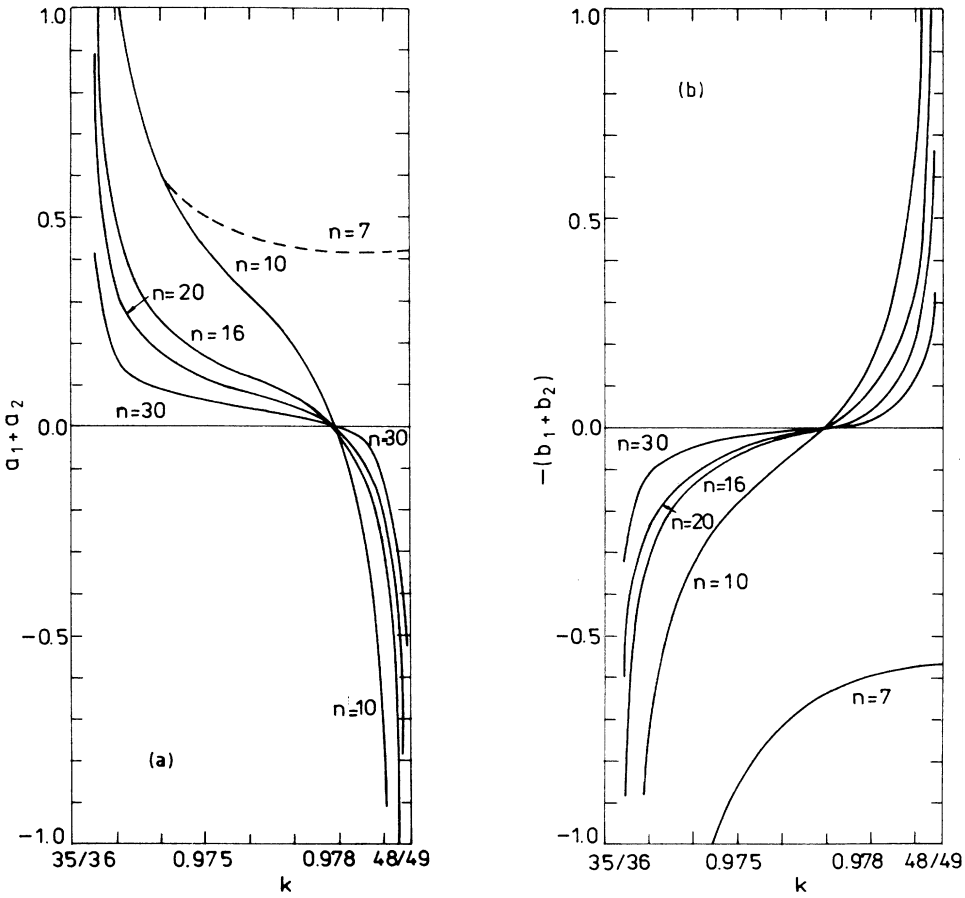

FIG. 6. (a) Same as 1(a), but for $0.972<k<0.9796$. For $n=7$ (dashed curve) the function represented is $\frac{3}{10}(a_1+a_2)$. (b) Same as 1(b), but for $0.972<k<0.9796$.

TABLE I. Two-photon transparency energies for several 1s-ns and 1s-nd transitions, in the energy region $0.375 \leq k \leq 0.984$.

k	0.375–0.75	0.75–0.8889	0.8889–0.9375	0.9375–0.96	0.96–0.972	0.972–0.9796
1s-3s	0.6936					
1s-4s	0.6912	0.8714				
1s-4d		0.8381				
1s-5s	0.6905	0.8707	0.9299			
1s-5d		0.8307	0.9215			
1s-6s	0.6901	0.8705	0.9295	0.9560		
1s-6d		0.8274	0.9192	0.9529		
1s-10s	0.6897	0.8704	0.9294	0.9557	0.9697	0.9780
1s-10d		0.8232	0.9163	0.9510	0.9676	0.9767
1s-20s	0.6895	0.8703	0.9293	0.9557	0.9697	0.9780
1s-20d		0.8216	0.9160	0.9505	0.9672	0.9766
1s-∞s	0.6894	0.8703	0.9293	0.9557	0.9697	0.9780
1s-∞d		0.8211	0.9157	0.9503	0.9671	0.9765

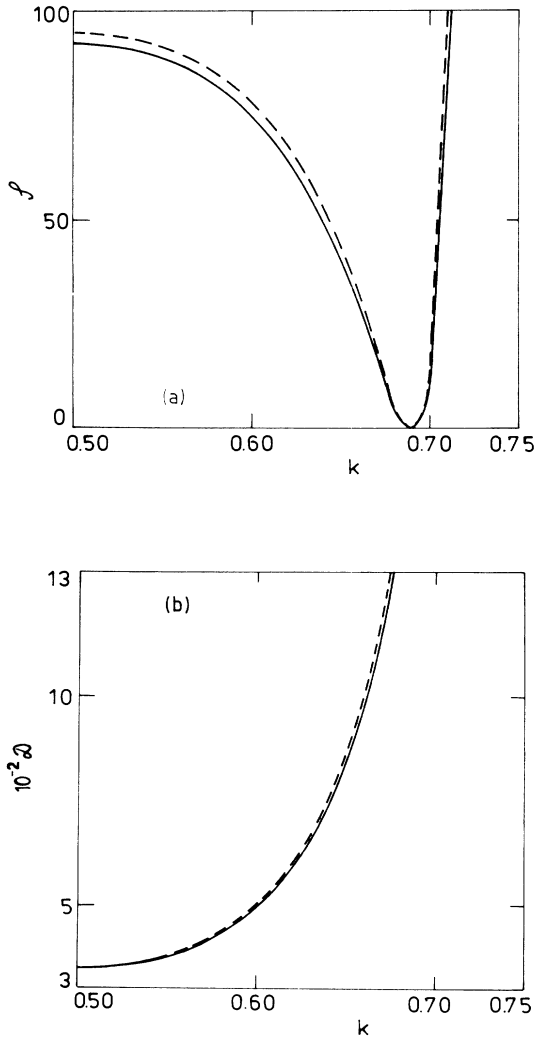

FIG. 7. The function $\mathcal{S}$ in Eq. (26) for $n=\infty$ (solid curve) and for $n=20$ (dashed curve) vs k, for $0.5<k<0.75$. (b) The function $\mathcal{D}$ in Eq. (27) for $n=\infty$ (solid curve) and for $n=20$ (dashed curve) vs k, for $0.5<k<0.75$.

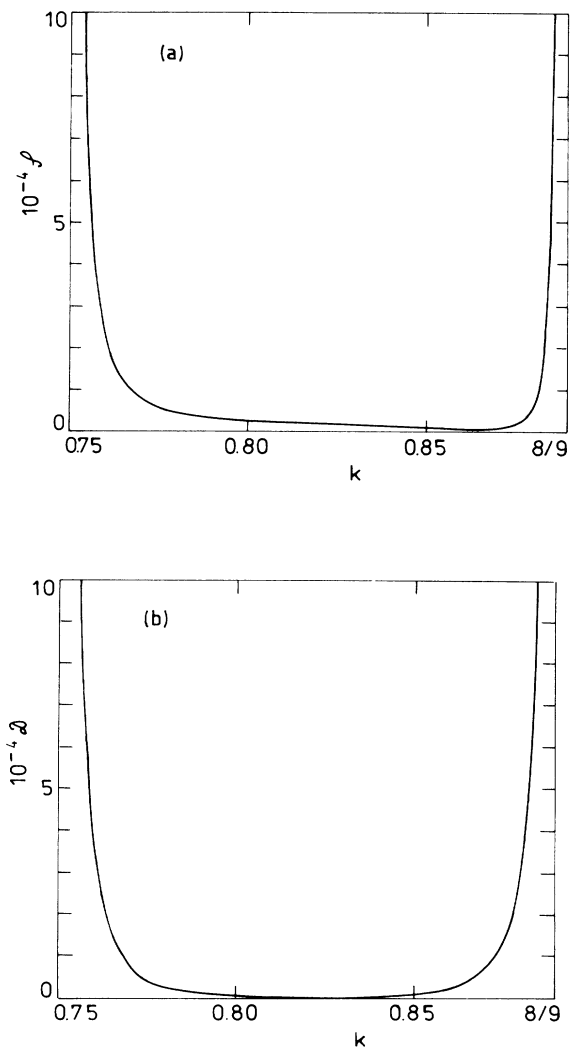

FIG. 8. (a) The function $\mathcal{S}$ in Eq. (26) for $n=\infty$ vs k, for $0.75<k<0.8889$. (b) The function $\mathcal{D}$ in Eq. (27) for $n=\infty$ vs k, for $0.75<k<0.8889$.

ϕ_1 is the Humbert confluent hypergeometric function [see (A3) and (A4)]. From Eq. (18) one deduces that $n^{3/2}a(1)$ and $n^{3/2}b(1)$ have finite limits for $n\to\infty$, in agreement with (21) and (22) taken for $\tau=1$, while $n^{3/2}a(n)$ and $n^{3/2}b(n)$ go to infinity.

The functions expressed by (22) have the same trend in their dependence on the photon energy as in the case of finite n: They become infinite for $\tau=N\geq 3$, having different signs on the two sides of a resonance.

IV. EMISSION AND ABSORPTION RATES

The measurable quantities are connected with the squared modulus of the Kramers-Heisenberg matrix element. In the emission case the primary quantity is the differential emission rate $d^3\Gamma_{i,f}$ from which one constructs the dimensionless quantity

$$\gamma_{if}\equiv\frac{d^3\Gamma_{i,f}}{d\omega_1 d\Omega_1 d\Omega_2}=\frac{r_0^2\omega_1\omega_2}{8\pi^3c^2}\,|\mathcal{M}_{i,f}|^2\,, \tag{24}$$

where r_0 is the classical electron radius, $d\omega_1$ a frequency interval, and $d\Omega_1$ and $d\Omega_2$ solid-angle elements. The energy of one of the photons is variable, while the energy of the second photon is given by (4). The emission rate (24) depends also on the photon directions and polarizations. From it one can obtain other different measurable quantities, explicitly shown in Sec. IV of Ref. 13, in which the indexes $3s$ and $3d$ have to be replaced now by ns and nd.

In the absorption case the basic quantity is the absorption rate

$$\frac{d^4\Gamma_{i,f}}{d\omega_1 d\omega_2 d\Omega_1 d\Omega_2}=\frac{(2\pi)^3}{\hbar}r_0^2\frac{c^4}{\omega_1^2\omega_2^2}\rho(\mathbf{k}_1,\mathbf{s}_1)\rho(\mathbf{k}_2,\mathbf{s}_2)$$

$$\times\,|\mathcal{M}_{i,f}|^2\delta(E_f-E_i-\hbar\omega_1-\hbar\omega_2)\,, \tag{25}$$

where $\rho(\mathbf{k},\mathbf{s})$ denotes the spectral density of the external

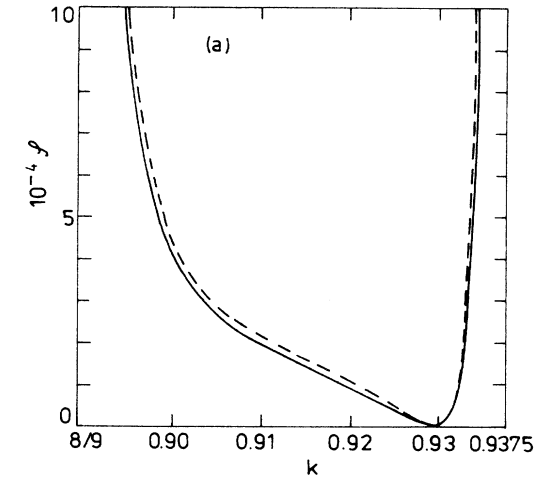

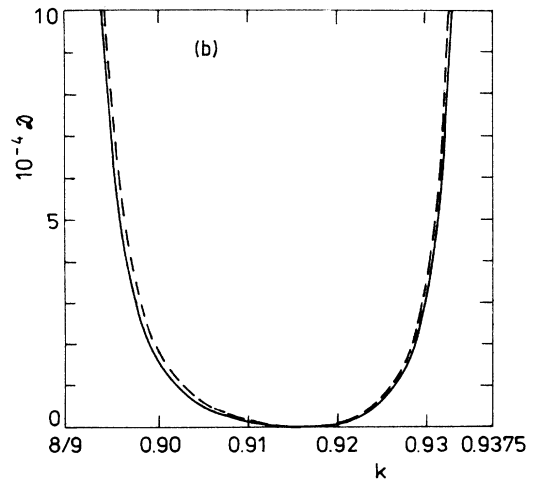

FIG. 9. (a) Same as 7(a), but for $0.8889<k<0.9375$. (b) Same as 7(b), but for $0.8889<k<0.9375$.

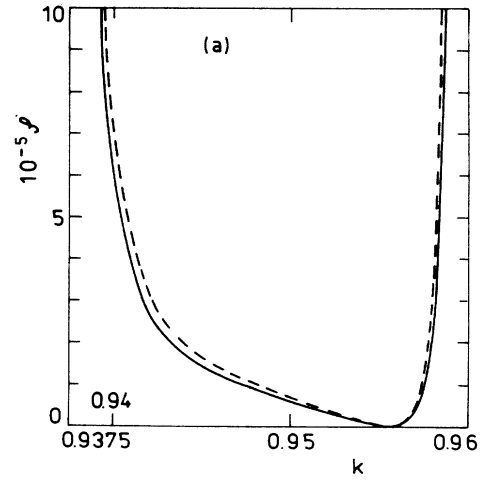

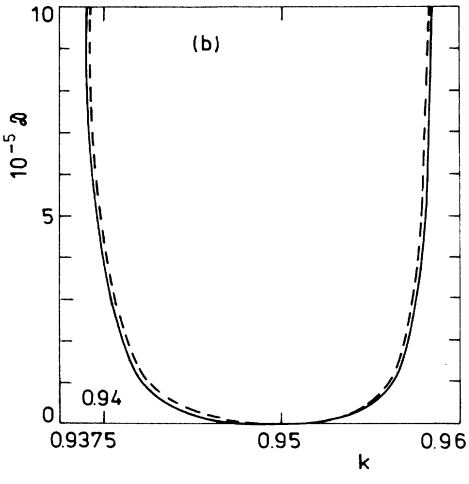

FIG. 10. (a) Same as 7(a), but for $0.9375<k<0.96$. (b) Same as 7(b), but for $0.9375<k<0.96$.

field analyzed over directions and polarizations. The total energy density is $\int_0^\infty \int_{k/k} \Sigma_s \rho(\mathbf{k},\mathbf{s}) d\Omega\, d\omega$, where $\omega = ck$. δ is the Dirac function, which appears in connection with the neglect of the energy level width.

V. NUMERICAL PROCEDURE AND RESULTS

Our numerical evaluation of the invariant amplitudes is based on Eqs. (14) and (15). We have found that the use of the expansion (A2) for the Appell functions F_1, which contains a number of Gauss functions of the order of the quantum number n, can be used without special problems for values of n as high as 50. The use of Kummer relation in order to change the variable x defined by (13) to $x_1 = x/(x-1)$ is advantageous because x_1 is a positive variable smaller than 0.5.

In the case of the limit $n \to \infty$, we have evaluated the Humbert functions in (22) with the expansion (A5). We have tested our codes by comparison with all the previous data available to us: the numbers of Quattropani *et al.*[11] for $6s$, $20s$, and $45s$ transitions, the numbers of Tung *et al.*[12] for $n = 3$, 4, and 6 (s and d transitions), and our numbers[13] for $n = 3$. The agreement was always in the limits of precision claimed by the different authors.

We found it convenient to represent the results for the invariant amplitudes in the second half of the photon spectrum [from the middle of the spectrum at $k = \frac{1}{2}(1 - 1/n^2)$ up to its end at $k = 1 - 1/n^2$], as done earlier in Ref. 11. In such a representation the position of the resonances is independent of n, in contrast to the situation in the first part of the spectrum. The resonances in the second part of the spectrum are located at $k_N = 1 - 1/N^2$, with $2 \le N \le n-1$. The end of the spectrum for the transitions $1s \to ns, nd$ is the last resonance for the transitions $1s \to (n+1)s, (n+1)d$.

We have studied systematically six regions of the photon energy defined in Eq. (17). The first region starts at $k = 0.375$, which is the middle of the spectrum for $n = 2$, and goes up to the first resonance for the transitions with $n \ge 3$, located at $k = 0.75$. For $n \ge 3$ this region also in-

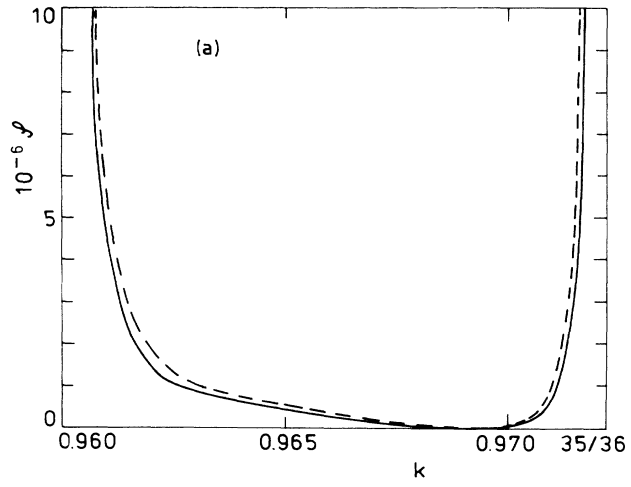

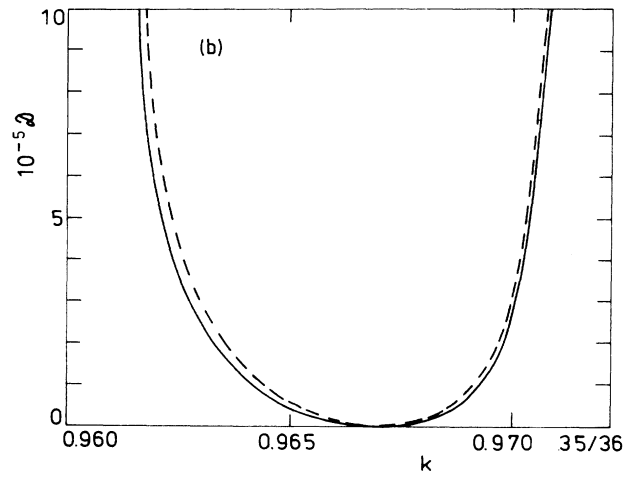

FIG. 11. Same as 7(a), but for $0.96 < k < 0.972$. (b) Same as 7(b), but for $0.96 < k < 0.972$.

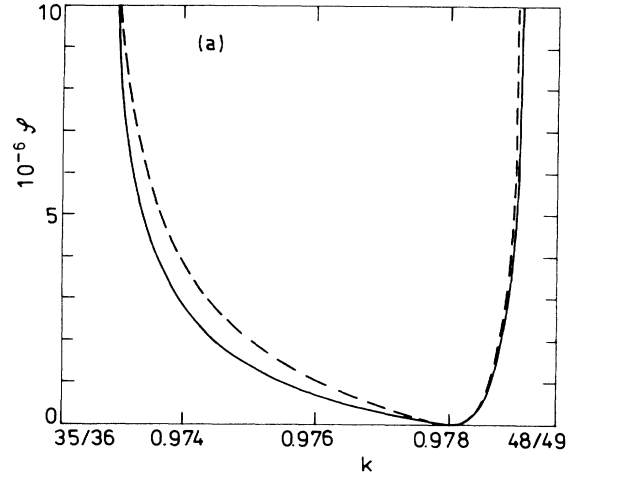

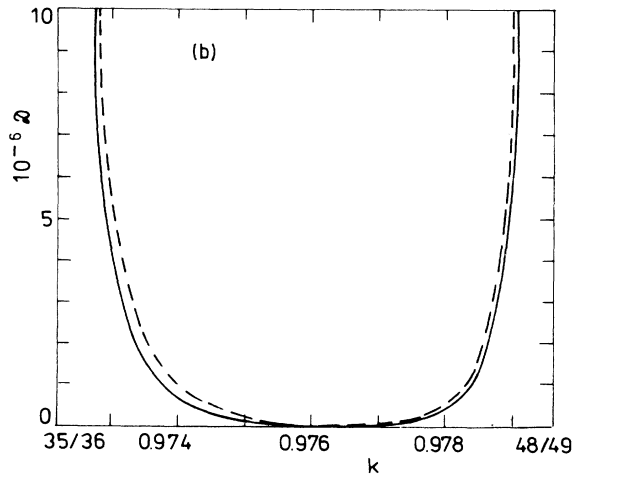

FIG. 12. (a) Same as 7(a), but for $0.972 < k < 0.9796$. (b) Same as 7(b), but for $0.972 < k < 0.9796$.

cludes a portion from the first part of the spectrum, namely, the region from 0.375 to $\frac{1}{2}(1-1/N^2)$. The other five regions continue the first one, extending from a resonance to the next one.

Our results are presented as graphs. Figures 1(a)–6(a) give the dependence of a_1+a_2 in Eq. (10), and Figs 1(b)–6(b) that of b_1+b_2 in Eq. (11), on the variable k for several values of n. In the first energy region (Fig. 1) the values of n are 3, 4, 5, 6, 10, and 16. The case of $n=20$ is included in the other regions, and also $n=30$ in the last two energy regions (Figs. 5 and 6). We mention that our results for 1*s*-*nd* transitions with $n>6$ are completely new, and that in the cases investigated previously in the literature the energy region explored was usually less extended than in our case.

Our graphs show some general features of the sum of the invariant amplitudes (a_1+a_2 in the *ns* case, b_1+b_2 in the *nd* case): (i) a monotonous behavior from one resonance to another, with a change of sign at each resonance; (ii) the existence of a transparency in each region with the following exceptions: *nd* transitions in the first energy region [see Fig. 1(b)], all transitions in the energy region between the last resonance and the end of the spectrum; (iii) a not too strong dependence of n, especially in the first regions; and (iv) in the last energy region for a given transition, its amplitude differs much more from the others than in the previous regions (compare the situation of $n=5$ in Figs. 4(a) and 4(b) to its situation in Figs. 1–3, or notice the situation of $n=7$ in Fig. 6).

We have determined numerically the position of the *transparencies* in the six photon-energy regions studied. The results are contained in Table I. For $n>10$ the position of the transparency is practically n independent. The last two lines, corresponding to the limit $n=\infty$, were obtained from a calculation based on Eqs. (21)–(23). As remarked by Tung *et al.*[12] for small values of n, the position of the transparency is different for *ns* and *nd* transitions in the first energy region.

Our results concerning the limit case $n=\infty$ are contained in Figs. 7–12. We have considered the same dimensionless functions as Quattropani *et al.*,[11] namely,

$$\mathcal{S}\equiv\frac{9}{k_1^2k_2^2}n^3\,|\,a_1+a_2\,|^2\,, \tag{26}$$

$$\mathcal{D}\equiv\frac{9}{k_1^2k_2^2}n^3\,|\,b_1+b_2\,|^2\,, \tag{27}$$

where $k_1=k$ and $k_2=1-1/n^2-k_1$ are the photon energies measured as indicated in Eq. (17). In Figs. 7(a)–12(a) we have represented the function $\mathcal{S}$, and in Figs. 7(b)–12(b) the function $\mathcal{D}$, in the limit $n=\infty$. They were evaluated with Eqs. (21)–(23). In Figs. 7 and 9–12 we present also the values of the function $\mathcal{S}$ or $\mathcal{D}$ for $n=20$ (dashed curves). We can see that the relative differences between $\mathcal{S}$ and $\mathcal{D}$ for $n=20$ and for $n=\infty$ are usually smaller than 10%. In the first two energy regions the differences are much smaller than in the other cases; the case $n=20$ is not shown in Fig. 8. With increasing photon energy, the relative differences between the compared quantities increase. Nevertheless, we think that a tabulation of the functions $\mathcal{S}$ and $\mathcal{D}$ for $n=\infty$ would allow useful conclusions about the functions $\mathcal{S}$ and $\mathcal{D}$ for $n>20$.

ACKNOWLEDGMENT

The authors thank Tudor Marian from the University of Bucharest for useful discussions.

APPENDIX A: EXPANSIONS FOR THE APPELL FUNCTION F_1 AND THE HUMBERT FUNCTION ϕ

For $|x|<1$ and $|y|<1$ the function F_1 is given by the double series[25]

$$F_1(\alpha,\beta,\beta',\gamma;x,y)=\sum_{m=0}^{\infty}\sum_{n=0}^{\infty}\frac{\alpha_{m+n}\beta_m\beta'_n}{\gamma_{m+n}1_m1_n}x^my^n\,, \tag{A1}$$

where $\alpha_m\equiv\Gamma(\alpha+m)/\Gamma(\alpha)$. For $|y|<1$ one has the expansion

$$F_1(\alpha,\beta,\beta',\gamma;x,y)=\sum_{m=0}^{\infty}\frac{\alpha_m\beta'_m}{\gamma_m1_m}y^m\,{}_2F_1(\alpha+m,\beta,\gamma+m;x)\,. \tag{A2}$$

A relation useful for the limit $n\to\infty$ presented in Sec. III is[25]

$$F_1(\alpha,\beta,\beta',\gamma;x,y)=\sum_{m=0}^{\infty}\frac{\alpha_m\beta'_m}{\gamma_m1_m}(y-x)^m\times{}_2F_1(\alpha+m,\beta+\beta'+m,\gamma+m;x)\,. \tag{A3}$$

For $|x|<1$ the Humbert confluent hypergeometric function is represented by the double series[25]

$$\phi_1(a,b,c;x,y)=\sum_{m=0}^{\infty}\sum_{n=0}^{\infty}\frac{a_{m+n}b_m}{c_{m+n}1_m1_n}x^my^n\,. \tag{A4}$$

It can be written also as

$$\phi_1(a,b,c,;x,y)=\sum_{n=0}^{\infty}\frac{a_n}{c_n}\frac{y^n}{1_n}\,{}_2F_1(a+n,b,c+n;x)\,. \tag{A5}$$

The last expansion is valid in the whole complex plane of the variable x except the region $(1,\infty)$ of the real axis.

APPENDIX B: DETAILS ON THE LIMIT $\tau\to n$

When $\tau\to n$ the products $(n-\tau)^{n-3}S_j$, with $j=1$ and $j=3$, and $(n-\tau)^{n-2}S_2$, where S_j is defined by Eq. (12), are finite. They can be evaluated using the expression (A2) for the Appell functions, which reduces to a sum of $(n-2)$ Gauss functions

$$S_j=\sum_{p=0}^{n-3}\frac{1}{1-\tau+j+p}\frac{(3-n)_p}{1_p}y^p\times{}_2F_1(1-\tau+j+p,3+n,2-\tau+j+p;x)\,.$$

For $\tau\to n$ the Gauss functions are finite, even for

$p=n-2-j$, because the variable x defined by (13) goes to zero. The variable y goes to infinity, but its increase is compensated by an adequate power of $(n-\tau)$. In the case of $j=1$ and 2 only the last term in the series contributes, while in the case of $j=3$ the last two terms have to be retained. We get in this way:

$$\lim_{\tau\to n}\left[\frac{n-\tau}{n+\tau}\right]^{n-3} S_1=\frac{-3n^2-4n+3}{2n(1+n)}\left[\frac{n-1}{n+1}\right]^{n-3}, \tag{B1}$$

$$\lim_{\tau\to n}\left[\frac{n-\tau}{n+\tau}\right]^{n-2} S_2=\frac{1}{2n}\left[\frac{n-1}{n+1}\right]^{n-3}, \tag{B2}$$

$$\lim_{\tau\to n}\left[\frac{n-\tau}{n+\tau}\right]^{n-3} S_3=\frac{-3n^2+4n+3}{2n(1-n)}\left[\frac{n-1}{n+1}\right]^{n-3}. \tag{B3}$$

With Eqs. (B1)–(B3) replaced in Eqs. (14) and (15), one obtains the expressions (19) for the invariant amplitudes at $\tau=n$.

APPENDIX C: THE VICINITY OF RESONANCES

As mentioned in Sec. II, if we do not include the finite widths of the energy levels, the invariant amplitudes a and b [Eqs. (14) and (15)] become infinite for Ω equal to an energy eigenvalue situated between E_1 and the final energy E_n. The behavior of the amplitudes in the vicinity of a resonance can be obtained from Eqs. (14) and (15), or directly from the starting expression (2) of the Kramers-Heisenberg matrix element, in which the Green function is expressed by its expansion in terms of energy eigenfunctions. After simple transformations (the replacement of the matrix elements of the operator $\mathbf{P}$ by those of $\mathbf{r}$, and the performance of the angular integrals), Eq. (2) leads to

$$a(\tau)=-\frac{m_e}{3\hbar^2}\sum_{\substack{n'(\geq 2)\\(n'\neq n)}}\!\!\!\!\!\!\int \frac{(E_{n'}-E_n)(E_1-E_{n'})}{E_{n'}-\Omega}R_{n0}^{n'1}R_{10}^{n'1}, \tag{C1}$$

$$b(\tau)=-\frac{2m_e}{15\hbar^2}\sum_{\substack{n'(\geq 2)\\(n'\neq n)}}\!\!\!\!\!\!\int \frac{(E_{n'}-E_n)(E_1-E_{n'})}{E_{n'}-\Omega}R_{n2}^{n'1}R_{10}^{n'1}. \tag{C2}$$

The sum is extended over the energy spectrum of the hydrogenlike atom (discrete and continuum). $R_{nl}^{n'l'}$ denotes the matrix element of r in the notations of Ref. 26. One of the methods used in the study of $1s\to ns$ transitions (see Ref. 11) was the numerical evaluation of an expression identical (up to a factor) to Eq. (C1).

We mention also that by standard manipulations one can transform a and b as

$$a(\tau)=\frac{1}{3}\frac{m_e}{\hbar^2}\left[\left[\Omega-\frac{E_1+E_n}{2}\right]S_{10,n0}-(E_1-\Omega)(E_n-\Omega)T_{10,n0}(\Omega)\right], \tag{C3}$$

$$b(\tau)=\frac{2}{15}\frac{m_e}{\hbar^2}\left[\left[\Omega-\frac{E_1+E_n}{2}\right]S_{10,n2}-(E_1-\Omega)(E_n-\Omega)T_{10,n2}(\Omega)\right], \tag{C4}$$

where

$$S_{nl,n'l'}\equiv\int_0^\infty r^4R_{nl}R_{n'l'}dr$$

and

$$T_{10,nl}(\Omega)\equiv\sum_{n''}\!\!\!\!\!\!\int\frac{R_{n''1}^{10}R_{n''1}^{nl}}{E_{n''}-\Omega}. \tag{C5}$$

When work is performed in the length gauge, the main quantities to be evaluated are the amplitudes $T_{10,nl}$.

In the vicinity of $\Omega=E_N$ only the contribution of the term with $E_{n'}=E_N$ is important in (C1) and (C2) and, consequently,

$$a(\tau)\simeq\frac{(n^2-N^2)(N^2-1)}{12(\tau-N)Nn^2}R_{n0}^{N1}R_{10}^{N1}, \tag{C6}$$

$$b(\tau)\simeq\tfrac{2}{5}a(\tau)R_{n2}^{N1}/R_{n0}^{N1}. \tag{C7}$$

In the above equations we made explicit the dependence on the variable τ, connected with Ω by Eq. (8). To $\Omega=E_N$ corresponds $\tau=N$. According to Eq. (16) this corresponds to the photon energies $k=1/N^2-1/n^2$ (when $\tau_2=N$) and $k=1-1/N^2$ (when $\tau_1=N$). The first set of energies is located in the first half of the spectrum and the other set in the second half.

The matrix element R_{10}^{N1} in Eq. (C6) has a simple expression. The other matrix elements can be evaluated from the general formula given in Ref. 26. We write here only the expressions of the amplitudes near the first resonance, corresponding to Ω in the vicinity of E_2 ($\tau=2$):

$$a\simeq-\frac{2^{12}}{3^5}\frac{n^2\sqrt{n}}{(n^2-4)^2}\left[\frac{n-2}{n+2}\right]^n\frac{1}{2-\tau}, \tag{C8}$$

$$b\simeq\frac{8}{5}\left[\frac{n^2-1}{n^2-4}\right]^{1/2}a. \tag{C9}$$

[1]R. Marrus and P. J. Mohr, Adv. At. Mol. Phys. **14**, 181 (1978).
[2]B. A. Zon, N. L. Manakov, and L. P. Rapoport, Zh. Eksp. Teor. Fiz. **55**, 924 (1968).
[3]M. Gavrila, Lett. Nuovo Cimento **2**, 180 (1969).
[4]S. Klarsfeld, Lett. Nuovo Cimento **2**, 543 (1969).
[5]L. P. Rapoport, B. A. Zon, and L. P. Manakov, Zh. Eksp. Teor. Fiz. **56**, 399 (1969).
[6]E. Karule, J. Phys. B **4**, L67 (1971).
[7]J. P. Gazeau, J. Math. Phys. **19**, 1041 (1978).
[8]M. Gavrila, Phys. Rev. **6**, 1360 (1972).

[9]E. Arnous, S. Klarsfeld, and S. Wane, Phys. Rev. A **7**, 1559 (1973).
[10]E. Karule, J. Phys. B **11**, 441 (1978); **18**, 2207 (1985).
[11]A. Quattropani, F. Bassani, and S. Carillo, Phys. Rev. A **25**, 3079 (1982).
[12]J. H. Tung, X. M. Ye, G. J. Salamo, and F. T. Chan, Phys. Rev. A **30**, 1175 (1984).
[13]V. Florescu, Phys. Rev. A **30**, 2441 (1984).
[14]V. Florescu and T. Marian, Central Institute of Physics, Bucharest, Report No. FT-245-1984 (unpublished).
[15]M. Luban, B. Nudler, and I. Freund, Phys. Lett. **47A**, 447 (1974).
[16]A. Costescu, I. Brandus, and N. Mezincescu, J. Phys. B **18**, L11 (1985).
[17]I. Freund, Phys. Rev. A **7**, 1849 (1973).
[18]Y. Bannett and I. Freund, Phys. Rev. Lett. **49**, 539 (1982); Phys. Rev. A **30**, 299 (1984).
[19]K. Ilakovac, J. Tudorić-Ghemo, B. Bušić, and V. Horvat, Phys. Rev. Lett. **56**, 2469 (1986).
[20]X. Mu and B. Craseman, Phys. Rev. Lett. **57**, 3039 (1986).
[21]V. Florescu and T. Marian, Phys. Rev. A **34**, 4641 (1986).
[22]We notice that the amplitude b here taken for $n=3$ differs by sign from the amplitude denoted by b in Ref. 13. This difference is without physical significance and comes from a difference in the sign of the $3d$ wave function in momentum space.
[23]The correspondence between a_1+a_2 in Eq. (10) and the amplitude D_1^n in Ref. 11 is $a_1+a_2=-\frac{1}{3}k_1k_2D_1^n$, where k_1 and k_2 are the photon energies measured as in Eq. (17).
[24]T. Marian (unpublished).
[25]P. Appell and J. Kampé de Fériet, *Fonctions Hypergéometriques et Hypersphériques* (Gauthier-Villars, Paris, 1926).
[26]H. A. Bethe and E. E. Salpeter, *Quantum Mechanics of One- and Two-Electron Atoms* (Springer, Berlin, 1957), Sec. 8.